ELSEVIER

Ceramics International 26 (2000) 579–582

CERAMICS INTERNATIONAL

Si_3N_4–Al_2O_3–TiC–Y_2O_3 composites intended for the edges of cutting tools

M. Szafran [a], E. Bobryk [a], D. Kukla [b], A. Olszyna [b,*]

[a] *Warsaw University of Technology, Faculty of Chemistry, Noakowskiego 3, 00-664 Warsaw, Poland*
[b] *Warsaw University of Technology, Faculty of Material Science and Technology, Narbutta 85, 00-524 Warsaw, Poland*

Received 26 May 1999; received in revised form 7 June 1999; accepted 18 September 1999

Abstract

This paper is concerned with the synthesis of composites in the Si_3N_4–Al_2O_3–TiC–Y_2O_3 system. The materials obtained have a high density and a good fracture toughness ($K_{IC} = 9.3$ MPa$\sqrt{m}$). Machining tests show that the service life of the tool blades made of these composites may even be tenfold longer than that of commercial blades made of Si_3N_4 with an additon of Al_2O_3, MgO and Y_2O_3.

Keywords: Si_3N_4–Al_2O_3–TiC–Y_2O_3 composites; E. Cutting tools

1. Introduction

Silicon nitride ceramics are promising candidates for engineering and tooling applications because of the combination of the excellent intrinsic mechanical, thermal and chemical properties [1]. Since the Si–N bonds in these materials have mostly the covalent character and, thus, the diffusion coefficients are small, silicon nitride is difficult to sinter. An efficient method of producing pore-less silicon nitride ceramic materials consists of introducing active additives during the sintering process and using pressure enhanced densification techniques, such as hot pressing (HP) or isostatic hot pressing (HIP) [2–4].

At the sintering temperatures, the densification facilitating substances, chiefly oxides such as Al_2O_3, Y_2O_3, MgO, CeO_2, ZrO, BeO and lanthanum oxides, react with the surfaces of the Si_3N_4, grains forming a liquid phase, which makes possible mass transport processes and enhances the densification [5–7]. The Si_3N_4, sintering activating additive most frequently used recently is a mixture of $Al_2O_3 + Y_2O_3$, since the sinters obtained with it have relatively best mechanical properties at high temperatures [8–10].

Si_3N_4, is also a well-known structural material both as a monolith and as a constituent of a composite [11]. Typically, in a densified monolithic form, Si_3N_4, is composed of α-Si_3N_4, containing elongated particles of β-Si_3N_4, in which the densification proceeds through debonding between the Si_3N_4 grains and through crack bridging by the β-phase. Si_3N_4, is also used in particulate-reinforced composites where interface debonding is essential for a high density [12].

The aim of the present study was to produce hard composite ceramic materials composed of Si_3N_4–Al_2O_3–Y_2O_3 and 10–30 wt% of TiC as the reinforcing phase. The method used in the experiment resorts to the known idea of increasing the fracture toughness (K_{IC}) of composite materials by introducing a certain amount of a phase with a substantially higher thermal expansion coefficient. This additional phase may be TiC whose expansion coefficient is relatively high whereas α for Si_3N_4, 3.2×10^{-6} 1/K.

2. Experimental procedure

The starting powders — silicon nitride, yttria, titanium carbide (MBE Industries, Yamaguchi, Japan) and alumina (ALCOA-Chemicals Division, US) were milled (40 h) using alumina milling balls, with ethanol alcohol as the milling medium. The compositions of the studied

* Corresponding author. Fax: +48-22-484-875.
E-mail address: aolszyna@meil.pw.edu.pl (A. Olszyna).

0272-8842/00/$ - see front matter
PII: S0272-8842(99)00098-X

Table 1
Compositions of the sintered samples

Composition	Si_3N_4 wt%	$Al_2O_3 + Y_2O_3$ wt%	TiC wt%
A	60	10	30
B	60	20	20
C	60	30	10

Table 2
Machining parameters

Cutting speed	$v = 2.5$ m/s
Feed	$f = 0.4$ mm/rev
Cutting depth	$ap = 1.0$ mm
Cutting lubricant	Dry machining

Table 3
Properties of the Si_3N_4–Al_2O_3–TiC–Y_2O_3 materials

Composition	Relative density (%)	Open porosity (%)	Closed porosity (%)	Hardness HV (GPa)	K_{IC} (MPa$\sqrt{m}$)
A	89.5	0.17	10.35	11.2	7.5
B	94.5	0.85	4.30	13.7	8.1
C	99.2	0.47	0.33	14.1	9.3

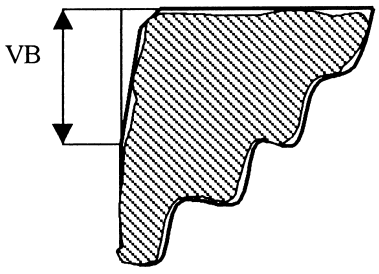

Fig.1. Flank wear of a ceramic tool blade — VB.

samples are given in Table 1. Then, the powder mixtures were dried, sieved and densified with a cylinder shape (20 mm in diameter, 20 mm high) by cold pressing (100 MPa) and cold isostatic pressing at a pressure of 250 MPa. The cylindrical samples were then hot-pressed (HP) in an induction-heated graphite die at a temperature of 1953 K under a pressure of 20 MPa for 0.5 h. The heating and cooling rates were 10 K/min.

The final density was evaluated by the Archimedes method, and the phases were identified by X-ray diffraction (XRD) using the CuK radiation. The density of the powder mixture was determined with a Accu Pyc 1330 type helium pycnometer. The chemical composition was examined using an X-ray microanalyser. Samples intended for microstructural observations and for mechanical measurements were ground and then polished with a 1/4 μm diamond paste. The morphology of the sintered material was examined by scanning electron microscopy (SEM). The hardness was determined using a Vickers diamond indenter under a load of 100, 300, 500 N and the fracture toughness by the indentation method using the equation formulated by Niihara et al. [13]. We also examined the machining indices of the Si_3N_4–Al_2O_3–Y_2O_3–TiC ceramics. The samples were prepared in the form of plates sized at 12×12×5 mm. The wear of the cutting blades was examined during a cutting operation (the parameters are given in Table 2) using a heat-treated carbon steel roller whose hardness was 25 ±1 HRC. The wear of the blades was determined by measuring the wear depth on the flank face VB (Fig.1). For the sake of comparison, we also measured the wear of commercial Si_3N_4–Al_2O_3–MgO cutting blades using the same method. The temperature within the cutting area as a function of the time of the

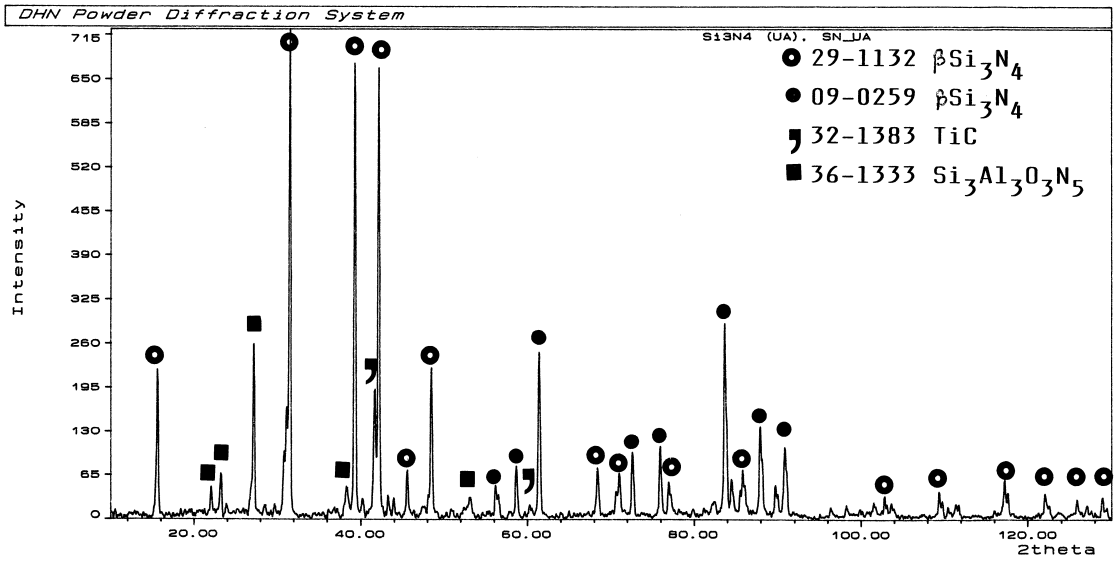

Fig. 2. XRD spectra of the Si_3N_4–Al_2O_3–Y_2O_3–TiC materials (C).

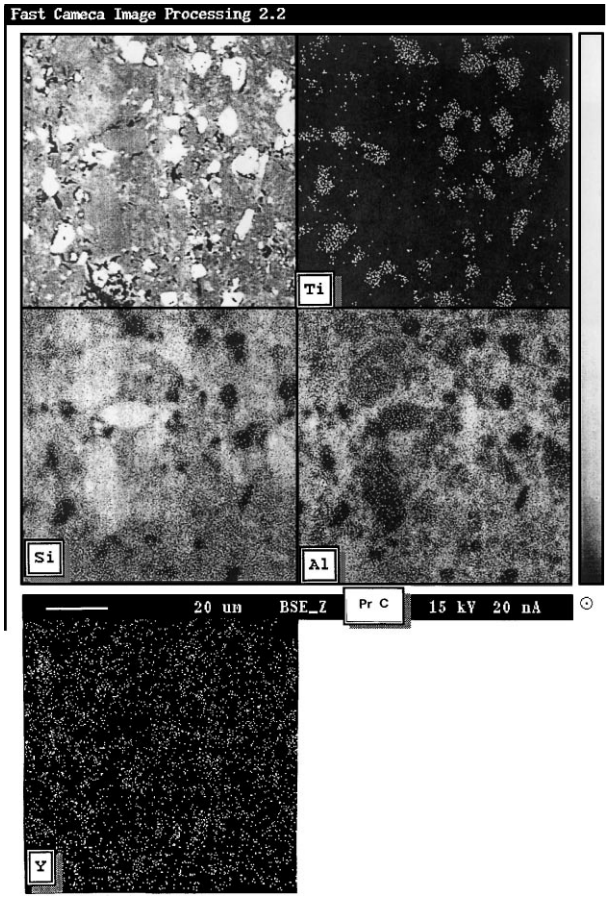

Fig. 3. An analysis of the chemical composition of the Si_3N_4–Al_2O_3–Y_2O_3–TiC materials (C).

blade operation was measured with a Thermalert pyrometer (Alborn, USA).

3. Results and discussion

The measured values of the densities, porosities, hardnesses and K_{IC} are given in Table 3. The relative density of the materials increases with increasing Al_2O_3, content and, in the mixture C (10 wt% TiC), reaches a value of 99.2%. The porosity, open and closed, varies in a similar way. It is interesting that the hardness of the composites falls within the range from 11.2 to 14.0 GPa, i.e. is relatively small compared with that known for Si_3N_4, (22 GPa), whereas the stress intensity factor K_{IC} reaches a value of 9.33 MPa (material C), which is substantially greater than the value known for Si_3N_4 (6.5–8.0 MPa).

Examinations of the phase composition of the materials (Fig. 2) have shown that a new phase, $Si_3Al_3O_3N_5$, forms during the sintering process. Its concentration increases with increasing share of Al_2O_3 in the powder mixture (the concentration of Y_2O_3 is constant). The Al_2O_3, and Y_2O_3 contents tend to zero and, finally, the material becomes a mixture of the β-Si_3N_4, TiC and $Si_3Al_3O_3N_5$, phases.

An analysis of the chemical composition (Fig.3) has shown that, on the surface of the materials, the TiC grains (8 μm in diameter on average) are uniformly distributed within the $Si_3Al_3O_3N_5$, matrix.

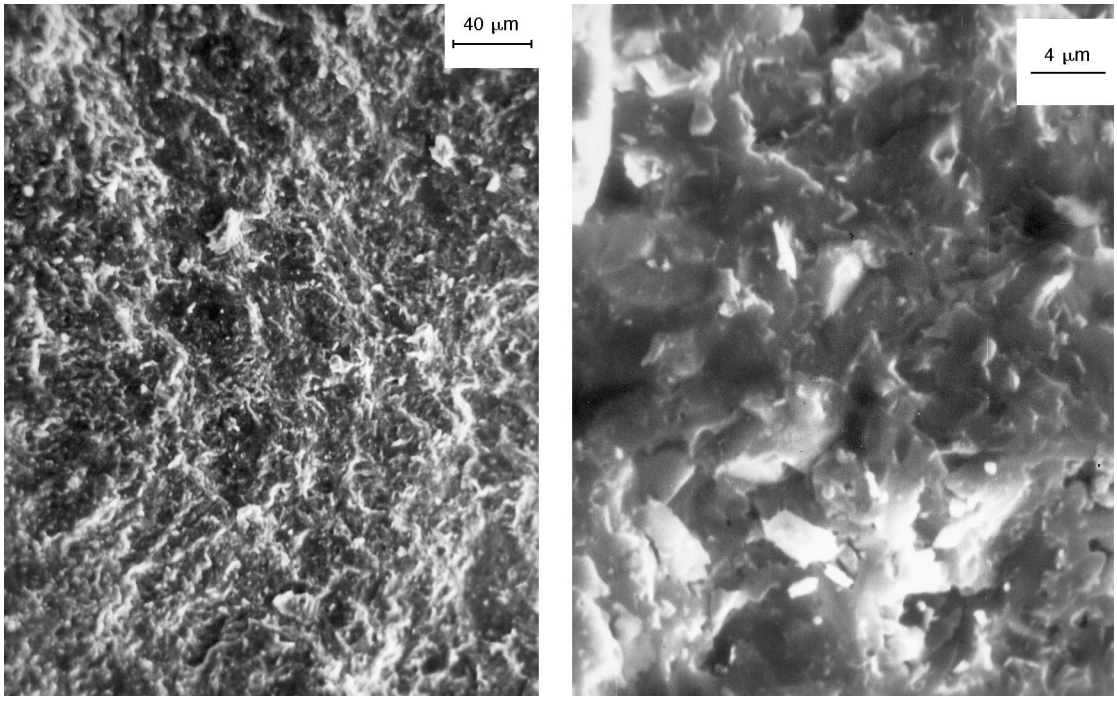

Fig. 4. SEM micrograph of the materials (C).

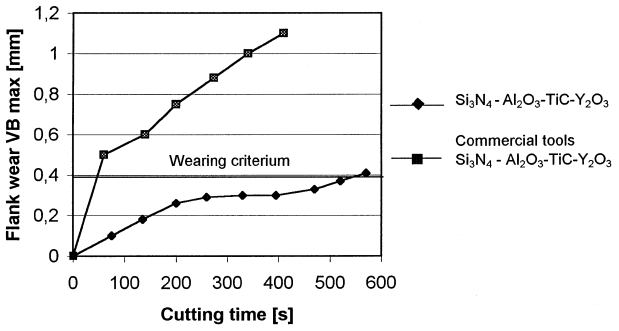

Fig. 5. Flank wear vs cutting time for Si_3N_4–Al_2O_3–Y_2O_3–TiC materials (A, B, C) and for commercial tools (Si_3N_4–Al_2O_3–Y_2O_3–MgO).

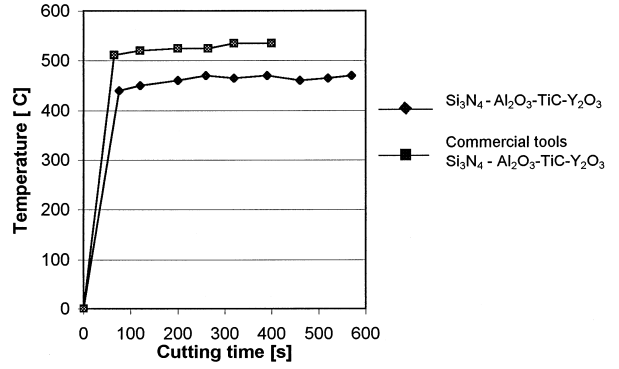

Fig. 6. Temperature within the machining region vs cutting time for Si_3N_4–Al_2O_3–Y_2O_3–TiC materials (A, B, C) and, for commercial tools (Si_3N_4–Al_2O_3–Y_2O_3–MgO).

Fig. 4 shows the morphology of the materials determined by the fracture technique. The microstructure appeared to be characteristic of materials with a very high relative density, in which the densification due to the sintering process leads to the formation of a liquid phase.

The variation of the wear of the plates A, B, C (30,20, 10 wt%TiC, respectively) and of the reference plate as a function of the machining time is shown in Fig. 5. We can see that the materials have very good machining properties. The durability of the plate C (the highest: relative density (99.2%), hardness (HV = 14.1 GPa) and stress intensity factor ($K_{IC} = 9.3$ MPa$\sqrt{m}$)) is tenfold the durability of the commercial Si_3N_4, reference plate. Fig. 6 shows the time variation of the temperature within the machining region. This curve is comparable in character (to within the measurement error) with that obtained for the reference tip, but the temperature values are lower.

4. Conclusions

The introduction of superhard TiC grains (HV = 30 GPa), intended to function as the reinforcing phase, into the Si_3N_4–Al_2O_3–Y_2O_3 composite increased both the hardness HV and the stress intensity factor K_{IC} of the material, thereby greatly improving its machining properties (compared to those of commercial Si_3N_4–Al_2O_3–Y_2O_3–MgO). Under the sintering conditions (temperature, time, pressure, atmosphere) employed in the present experiments, the maximum densification degree was achieved in sample C (10 wt%TiC), which manifested itself in the highest values of HV and K_{IC} and the best machining properties.

The results, presented above, concerning the synthesis and applications of the composites based on the Si_3N_4–Al_2O_3–Y_2O_3–TiC system indicate that this system is very promising as regards both its brittle fracture toughness and its machining properties. In view of their substantially longer service life and the lower temperature within the machining region, the cutting rods made of these materials seem to be higher over the tools made of Si_3N_4, added with small amounts of Al_2O_3, MgO and Y_2O_3.

References

[1] M.J. Hoffmann, G. Petzow, Tailoring of mechanical properties of Si_3N_4 ceramics, NATO ASI, Ser. E. 1994, pp. 276.
[2] C.G. Gniesin, I.I. Osipowa, Porosh. Metall 4 (1981) 32.
[3] J. Heinrich, E. Backer, M. Bohmer, J. Am. Ceram. Soc. 71 (1998) C28.
[4] G.R. Trewillger, F.F. Lange, J. Am. Ceram. Soc. 54 (1974) 25.
[5] I.H. Levis, R.J. Lumby, Powder Metall 26 (1983) 73.
[6] C. Kawai, A. Yamakawa, Crystal growth of silicon nitride whiskers through a VLS mechanism using SiO_2–Al_2O_3–Y_2O_3 oxides as liquid phase, Ceramics International 24 (1998) 135–138.
[7] J. Vleugles, P. Jacobs, J.P. Kruth, P. Vanherck, W.Du Mong, O. Van Der Biest, Machining of steel with sialon ceramics: influence of ceramics and workpiece composition on tool wear, Wear 189 (1995) 32–44.
[8] T. Hayashi, H. Hunakata, H. Suzuki, H. Sato, J. Mater. Sci. 21 (1986) 3501.
[9] N. Hirosaki, A. Okada, M. Mimoto, J. Mater. Sci. 25 (1990) 1872.
[10] J. Vleugels, O. Van der Biest, Machining of steel with sialon-bored composites, In: Proceedings of CIMITEC'98, World Ceramics Congress & Forum on New Materials, Florence, 14–19 June 1998, Italy.
[11] I.E. Reimanis, J.J. Petrovic, H. Suematsuand, T.E. Mitchell, J. Am. Ceram. Soc. 79 (1996) 395.
[12] P.F. Becher, J. Ceram Soc. 74 (1991) 255.
[13] K.A. Niihara, R. Morena, D.P.H. Hasselman, J. Mater. Sci. Letters 1 (1982) 282.